JOURNAL OF GEOPHYSICAL RESEARCH, VOL. 95, NO. B13, PAGES 21,805–21,821, DECEMBER 10, 1990

Analysis of Nuclear Explosion Salmon Free-Field Ground Motion Data for Nonlinear Attenuation

G. D. McCartor[1] AND W. R. Wortman

Mission Research Corporation, Santa Barbara, California

In order to assess the existence and impact of mild nonlinear contributions to the attenuation of seismic signals from underground explosions, free-field motion data from underground 5.3-kt nuclear test Salmon have been examined. These data, which were taken in a salt dome at ranges from 166 to 660 m, show moderate strains (10^{-3} to 10^{-4}) which may provide nonlinear attenuation. The attenuation over an order of magnitude in peak amplitude can be described approximately by an attenuation function Q of a bit less than 10; however, the calculated waveform using this constant Q is noticeably wider than the data. A linear but frequency dependent Q which decreases with decreasing frequency gives a reasonable fit to much of the waveform change as well as the peak amplitude decay with range. The higher-speed precursor which precedes the main pulse in the data cannot be described by this linear Q. With a spherical finite difference calculation driven by the 166-m Salmon pulse, it is found that a rapid shear modulus decrease at a 10^{-4} strain threshold can reproduce the observed precursor and other features of the pulses at greater ranges when a linear broad absorption band with $Q \approx 10$ is also added. The attenuation of the Salmon pulse thus can be attributed in part to a nonlinear effect of material failure as well as to a conventional linear mechanism. There are reasons to believe that the attenuation is not linear, but the Salmon data alone cannot verify this view.

Introduction

Near-field pulses from underground explosions certainly exhibit nonlinear behavior, at least out to a radius for which gross structural changes in the rock appear. Beyond this radius (roughly 100 m/kt$^{1/3}$) for strains less than 10^{-3}, but before linear level strains of 10^{-6} are reached, there may be subtler nonlinear changes that influence propagation. For the purposes of establishing a seismic source function [*Mueller and Murphy*, 1971; *Von Seggern and Blandford*, 1972; *Masse*, 1981], it is common to determine a range beyond which the pulse is taken as linear, as indicated by experimental data indicating a nearly constant reduced displacement potential. Typically, this "elastic radius" is taken at a few hundred m/kt$^{1/3}$. In relating teleseismic observations and implied source characteristics, it is assumed that the signal propagates linearly with some attenuation imposed in the form of a Q function. However, if there is significant contribution from nonlinear behavior, the resulting teleseismic waveforms may be in error. Here we examine the Salmon near-field data where the strains are in transition from highly nonlinear crushing to a linear regime that can be described by Q in order to identify any clear evidence of nonlinear behavior and to provide a description of the mechanism that produces it.

Previous Work

Of the large body of information available for the propagation of seismic signals in the intermediate strain regime, corresponding to strains varying from about 10^{-3} to about 10^{-6}, the data for salt appear to be the most nearly complete [*McCartor and Wortman*, 1985, 1988]. Data from the Salmon nuclear explosion [*Perret*, 1967; *Rogers*, 1966], the Cowboy series of chemical explosions [*Murphey*, 1961; *Minster and Day*, 1986; *Wortman and McCartor*, 1989], and *Larson*'s [1982] data on laboratory chemical explosions provide propagation data in the relevant strain regime for a wide range of yields (approximately 10 orders of magnitude), distances, and characteristic frequencies [*Trulio*, 1978]; the range of scaled distances (distance/yield$^{1/3}$) is a factor of about 300 while the range of characteristic frequencies is nearly 4 orders of magnitude. The propagation of pulses from explosions approximately satisfies cube root scaling: if distances and times are scaled by the cube root of the yield, the waveforms and amplitudes from all events are nearly the same even though at least some portion of the data is presumably in the nonlinear regime. Furthermore, the propagation provides a waveform which changes only slowly with distance.

Salt is a relatively uniform medium for which there are a variety of experiments ranging from Salmon through the Cowboy series to small laboratory explosions as reported by Larson. The experiments of Larson for small chemical explosions in pressed salt have provided pulses over a scaled range from 10 m/kt$^{1/3}$ to 200 m/kt$^{1/3}$. The dominant range of frequencies covered was from about 10^4 to 10^5 Hz, and the ratio of peak particle velocities to compressional sound speed (which is comparable with the strain) went from about 10^{-1} to less than 10^{-3}; by most standards this would suggest that the response was nonlinear. Yet, by performing a direct superposition experiment with a pair of simultaneous explosions, it was found that the resulting response was consistent with linear addition of the two narrow pulses of peak strain 10^{-3} as would be expected from a linear medium. Still it is not clear just how nonlinear effects would be manifest in this experiment without knowing the character of any nonlinear behavior. That is, the apparent success of superposition for pulses with large strains may not directly negate the possibility of any sort of nonlinear behavior (S. M. Day, private communication, 1989). The Cowboy series of chemical ex-

[1]Now at Department of Physics, Southern Methodist University, Dallas, Texas.

Paper number 90JB01920.
0148-0227/90/90JB-01920$05.00

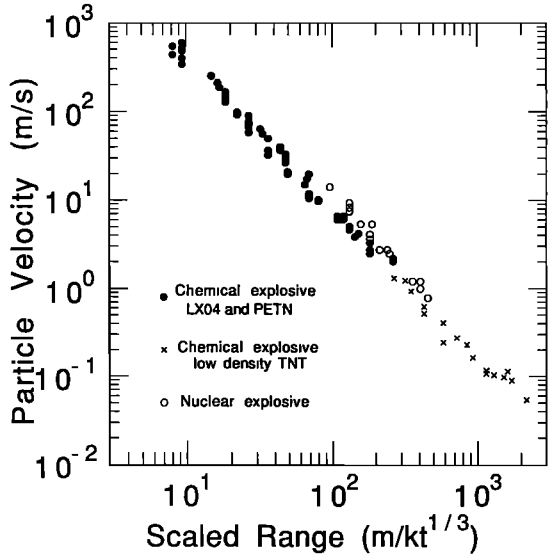

Fig. 1. Peak particle velocities from explosions in salt [from *Larson*, 1982].

plosions had a range of yields from 10 to 2000 lb (4.54 to 908 kg) of TNT, some of which were carried out in cavities for decoupling tests. The scaled ranges for the coupled experiments were from 200 to 3000 m/kt$^{1/3}$, and the corresponding peak strains were from a few times 10^{-4} to about 10^{-5}. The dominant frequencies were 10–10^2 Hz. The Salmon event took place in a natural salt dome; a comprehensive set of measurements were taken, both at surface and at subsurface locations. Subsurface measurements included scaled ranges from 100 m/kt$^{1/3}$ to about 425 m/kt$^{1/3}$, which provided peak strains from about 4×10^{-3} to about 3×10^{-4} with dominant frequencies from 1 to over 10 Hz. The Salmon data show remarkable internal consistency and correspond well with the other salt data.

Peak velocity data from the salt shots are shown as a function of scaled range in Figure 1. The scaled data from a huge range of yields tend to fall nearly on a straight line indicating a power law behavior with an exponent of about -1.9. This contrasts with a value of about -1.05 for pure elastic behavior for this waveform over this range when near-field ($1/r^2$) effects are included. Simple scaling with yield appears to hold over this great range of strains, approximately 10^{-1} to 10^{-5}. Note again that the range of yields over which simple scaling holds includes strains which are expected to give nonlinear behavior. However, deviation from r^{-1} behavior is not necessarily a nonlinear effect. In particular, linear but inelastic (i.e., anelastic) behavior can provide such results.

Trulio [1978] has noted that the Salmon data for decay of peak velocity with range are consistent with an effective Q of about 5. The effective Q for this process tends to increase with increasing frequency and with decreasing strain. Note that simple scaling, in conjunction with linearity, indicates that Q must be independent of frequency as well as amplitude. To some degree, dependence on both variables is subject to experimental examination. *Gupta and McLaughlin* [1989] have analyzed Salmon and Sterling data and concluded that the effective Q at Salmon strains appears to be mildly strain dependent with a Q of 5–10. Q is also larger at frequencies above the corner. Sterling data, which are at lower strains, are less cohesive, but they indicate a significantly larger Q, of over 300, consistent with a transition to a linear low attenuation at small strains. *Langston* [1983] indicates that Sterling S waves, generated by induced normal faulting, show a Q_β of about 35, suggesting a P wave Q of about 70. *Denny* [1990] reports that the source spectra characteristics of Salmon and Sterling indicate that the Salmon pulses are nonlinear to beyond 700 m.

Minster and Day [1986] have used the scaled peak velocity data for Cowboy to determine if these data require an amplitude (nonlinear) or frequency dependent Q for consistency. It is determined that a Q^{-1} which consists of a small constant plus a term proportional to the peak strain provides a good fit to the data when applied in a piecewise linear fashion. The observed attenuation effects do not firmly indicate the need for a frequency dependent Q, but they do indicate that an amplitude dependent Q provides a much more convincing fit than a constant Q. It is concluded that there must be nonlinear attenuation in the Cowboy strain regime. *Wortman and McCartor* [1989] analyzed the Cowboy data by using data pairs from individual shots. They also found a significant strain dependence in attenuation with a reduction in attenuation over strains of 10^{-4} to 10^{-5}.

Some data from laboratory explosions in pressed salt [*Larson*, 1982] show that three sensors at increasing ranges of 30–70 m/kt$^{1/3}$ provide increasing values of Q from 12 to 25. A constant Q cannot describe the results.

New England Research laboratory ultrasonic pulse propagation experiments [*Coyner*, 1987] have strains from less than 10^{-6} to more than 10^{-5}. In these experiments, compressional and shear ultrasonic pulses consisting of about two cycles at 100–200 kHz were propagated through samples. Attenuations were calculated using a spectral ratio technique. Variations of the attenuation with peak strain amplitude and confining pressure were determined. For dome salt it was found that over a strain range of 5×10^{-7} to 3×10^{-5} and for a confining load range of 0.1–1 MPa, the P wave attenuation is nearly constant and can be described by a Q of about 20. There is no particular evidence of nonlinearity in these data alone although the attenuation is large. It should be noted that these confining pressures are small compared with those for underground sources.

Laboratory data on the absorption of the energy in small oscillations of halite rods have been compiled by *Tittmann* [1983]. These experiments on decay of cyclic motion induced in salt samples indicate that for strains below 10^{-6}, and confining pressures consistent with that for underground explosions, a value of Q of several hundred is appropriate. For larger strains the value of Q decreases, indicating a nonlinear attenuation, although the nonuniform nature of the deformations in the experiment makes it difficult to extract Q as a function of strain.

These salt data generally indicate that for strains in excess of 10^{-5} there is an attenuation which is probably nonlinear, which increases with increasing strain, and which can be described by an effective Q of the order of 10 for the dominant frequencies in the pulses. No detailed knowledge of the attenuation mechanism currently exists, but there does appear to be a consistency in that the explosively generated pulses closely obey simple scaling, at least for peak velocities and corner frequencies, if not for all waveform details [*Trulio*, 1978; *Larson*, 1982]. This suggests that

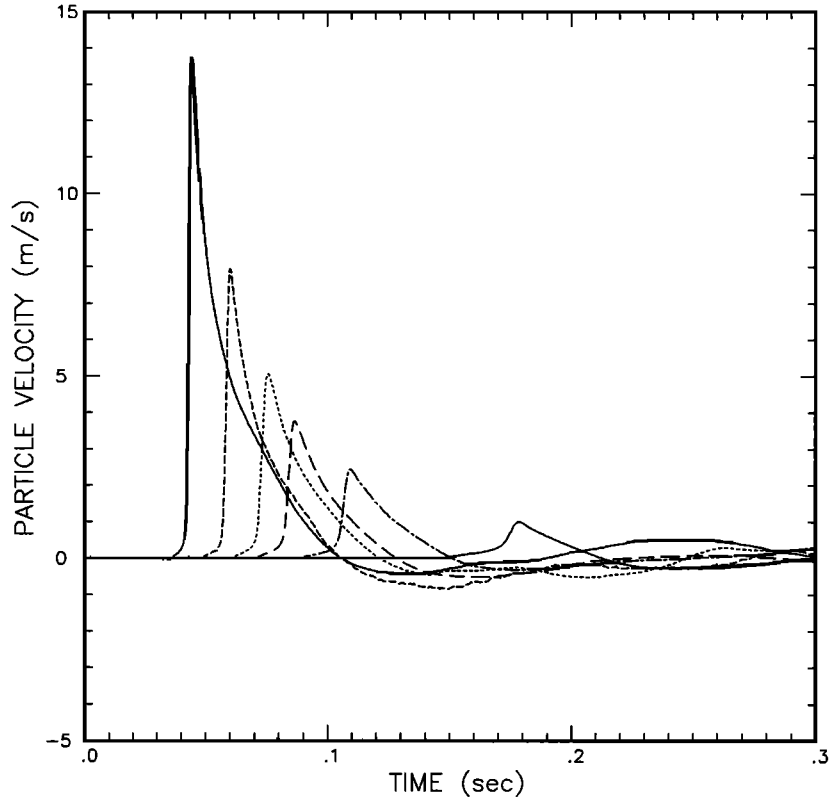

Fig. 2. Corrected Salmon velocity records at 166, 225, 276, 318, 402, and 660 m, in that order from left to right.

the mechanism must be rate independent. Data for strains near 10^{-6} are not so consistent, but they come from limited and diverse experiments. Generally, attenuation decreases to a modest level for strains less than 10^{-6} and then is presumably linear.

Salmon Data and Nonlinear Behavior

We shall now consider the extent to which Salmon data can shed light on the issue of linear versus nonlinear behavior beyond the "elastic radius" by exploring the consequences of the assumption of linear behavior. This will be done by examination of a series of velocity records from subsurface sensors to see if they are consistent with strictly linear behavior. We shall attempt to determine if the records exhibit features that cannot be understood in terms of linear attenuation which is possibly a function of frequency. If the data are consistent with attenuation which is independent of amplitude, but is possibly a function of frequency, they may allow the possibility that the propagation mechanism is linear without ruling out a nonlinear effect. However, even then such a restriction can serve to rule out a wide range of possible nonlinear mechanisms.

Salmon Data

As discussed in detail in Appendix A, the data records used in this analysis of Salmon are taken from five acceleration gages and one velocity gage all oriented in the horizontal plane and in the radial direction with respect to the working point. The selected records are corrected for baseline shifts and apparent clipping of the acceleration peaks. The acceleration records are expressed as velocities by integration. The velocity histories finally used are the apparent spherical radial values found by taking the measured cylindrical radial velocities and dividing by the cosine of the elevation angle from the working point to the gage. This assumes that the motion is along the radial from the working point and that the gages are properly oriented. The corrected velocity records finally used include those at ranges from 166 to 660 m, and they are shown in Figure 2. Some features of the more distant examples are difficult to appreciate fully when all records are plotted on the same scale. To clarify these features, the same data are plotted again in Figure 3, normalized to unit peak amplitude.

The records were selected so as to have the largest possible set with as many significant spatial separations as possible while also having them as internally consistent as possible. As discussed in Appendix A, this consistency was established by selecting records free of obvious waveform anomalies whose peak velocities fall along as smooth a curve as possible when plotted against range while following the trend of all the data. There is no real reason to believe that any individual one of the records selected is more desirable than some which were ignored. However, the resulting decay with range is consistent with all the scaled data from Figure 1. By selecting this data set, we hope to minimize the systematic effects of asymmetries, calibration and orientation errors, geological and grouting inhomogeneities, and additional but unknown sources of variation insofar as they mask the ideal smooth amplitude variation. However, we must obviously now avoid drawing conclusions which draw significantly on the details of the absolute amplitudes and concentrate on the effects of the trends of change and waveform variation.

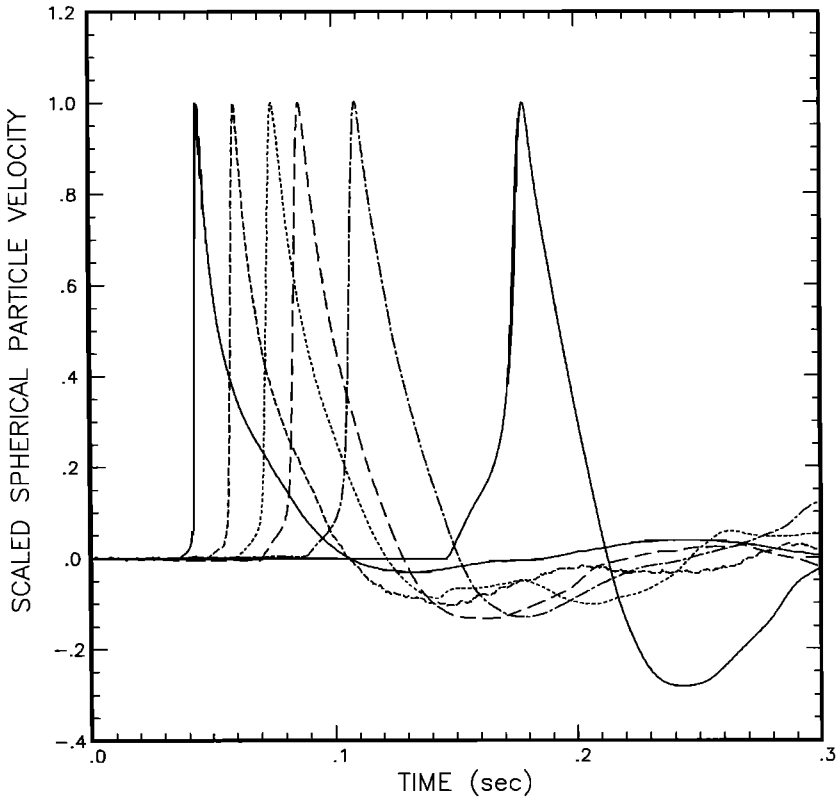

Fig. 3. Salmon velocity records normalized to unit peak amplitude.

A major motivation for using data whose amplitude changes smoothly is our application of the spectral ratio method to find an effective attenuation function as a function of frequency and range. If irregular fluctuations of overall amplitudes are included in waveforms, as might result from an instrument calibration error, the $1/Q$ function then determined from a pair of waveforms will be contaminated by an additional contribution inversely proportional to frequency. Of course, this means that any systematic change in the amplitude in the records (or selection of the records for particular properties) can give an artificial frequency dependency for the resulting attenuation. By taking data whose amplitude variation smoothly follows the trends of all Salmon data, as well as other scaled results, we hope to avoid such contamination.

Precursor

The Salmon data have a feature which may be useful in understanding some nonlinear effects of attenuation. Each of the pulses experimentally observed at six sensors at ranges from 166 m to 660 m exhibits a discontinuity in the slope upon the initial steep rise in pulse velocity, as seen in Figure 3. This appears as a toelike behavior in the leading edge of the velocity profile which has been described by *Perret* [1967] as an "elastic precursor" to the main pulse. The absolute amplitude of the toe remains approximately constant with range, at a particle velocity of about 0.5 m/s, while its amplitude relative to the peak increases with range. This precursor amplitude corresponds to a compressional strain level of $\varepsilon \approx 10^{-4}$ as inferred from the ratio of particle velocity to propagation speed. The leading edge of the pulses (i.e., that disturbance earliest in time) propagates at a speed of about 4.7 km/s while the pulse peaks, always after the toe, propagate at a speed of about 3.7 km/s. The elastic compressional speed of mild disturbances in this salt medium found from independent measurements were typically about 4.6 km/s. This indicates that the precursor signal seen in the Salmon data is due to elastic behavior while the subsequent pulse suffers a lower propagation speed because of some relaxation or plastic behavior.

Perret suggests that an elastic-plastic material behavior might account for the data in perhaps one of two ways. First, the precursor could develop at large strain, where an elastic limit is exceeded from radii much smaller than instrumented for Salmon, and continue to propagate in front of a following plastic wave. Second, it may be that the precursor develops in the moderate strain region if dome salt has an elasto-plastic nature at such strains. In either case the modulus of salt must be a function of the strain, that is, the medium is nonlinear.

If the precursor develops at large strain, there must be an elastic limit beyond which plastic behavior provides a lower modulus. When such a medium is dynamically loaded beyond the elastic limit, a leading pulse at the elastic limiting stress is generated followed by a larger amplitude but slower plastic wave. If the elastic-plastic transition is not sharply defined, the resulting pulse could consist of a gently rising leading elastic front which smoothly merges with the main plastic pulse much as seen in the Salmon data. Perret points out that if some energy from the plastic component is fed to the elastic portion during propagation, the amplitude of the elastic piece could remain nearly constant, but this is quite

speculative. What is known is that a variety of laboratory experiments show that strong impulsive sources can produce elastic precursors in a variety of media. For example, work of *Ahrens and Duvall* [1966], using planar pulses in quartz generated by explosives, exhibits an apparent elastic stress limit of about 70 kbar corresponding to strains of about 10^{-1}. This produces a leading edge, described as the elastic shock, which propagates at a speed in excess of that of the deformational portion of the pulse which follows. The elastic shock propagates with an equivalent modulus which is greater than the static modulus at this high stress. It is speculated that the elastic wave is supported by a higher than equilibrium shear stress. After the elastic component has passed, the shear stress is apparently reduced to the static value by a plastic or fracture process. This experiment, as well as that by *Taylor and Rice* [1963] which also shows an elastic precursor, provides elastic limits of many or tens of kilobars, in contrast with the Salmon data since they give a precursor amplitude of about 5 bars. Consequently, this mechanism does not seem a likely means of accounting for the Salmon precursor since it shows a nearly constant and small amplitude which seems to begin near the 166-m sensor range.

The second possibility indicated by *Perret* [1967] is that of having the precursor develop locally in the observation region on the basis of moderate strain plastic behavior. While there is no accepted dynamical equation of state for dome salt, Perret points out that dome salt is known to be highly plastic: under static conditions it is nearly hydrostatic. Thus plastic deformation of salt at moderate stresses is apparently normal. In order to account for the precursor data in Salmon, the equation of state would have to provide linear behavior up to a threshold (a threshold of about 5 bars, much less than the 70 kbars found for the elastic shock discussed above) and, through some deformation of the material, relax the modulus abruptly (on the Salmon time scale) to a value which provides a compressional propagation speed about 20% less than that for that infinitesimal strains in undisturbed material.

Data Analysis

Figure 3 indicates that the normalized pulse shape changes fairly slowly and smoothly, but there is a mild tendency to smooth out the sharp peak and to increase its width. These features suggest that the higher-frequency components are being more rapidly attenuated than the low-frequency components as would be appropriate, for example, with a constant Q, should such a description be suitable. Beyond this, there is the initial ramp or precursor on each pulse which strengthens relative to the peak amplitude as the radius increases. In order to establish the possible nonlinear character of the Salmon data, we shall adopt the position of exploring the consequences of the assumption of anelastic behavior as expressed in terms of a Q function which we shall attempt to evaluate. If this attempted description leads to contradictions, such as an effective Q that depends upon amplitude, we shall attribute the effects to nonlinear behavior. We shall use the data to make estimates of Q over a range of frequencies and amplitudes. Since we are dealing with data exclusively from a single event, no assumptions about the scaling behavior are necessary, and no such information will be gained.

A strict interpretation of anelastic behavior would require that we find a Q function, dependent generally upon frequency, as well as a compressional phase velocity c which is consistent with Q, so as to enforce the requirement of causality [*Aki and Richards*, 1980]. However, moderate values of Q are consistent with a nearly constant c, at least over the range of frequencies which are available to experimental verification. As indicated by *Kjartansson* [1979] and generalized to spherical geometry by *McCartor and Wortman* [1985], the propagation of a pulse in an anelastic medium with Q independent of frequency can be given analytically in the frequency domain as shown in Appendix B. This leads to representation of the change of the Fourier transform of the velocity in going from radius "a" to "r" as

$$\exp\left[\frac{-\omega(r-a)}{2cQ}\right] = \left|\frac{\bar{v}(r,\omega)}{\bar{v}(a,\omega)}\right| \left|\frac{(i\omega/ca) - (\omega/2cQa) - (1/a^2)}{(i\omega/cr) - (\omega/2cQr) - (1/r^2)}\right| \tag{1}$$

where c, a mild function of frequency, and Q are given by Kjartansson as discussed in Appendix B. This relation allows the testing of changes in velocity pulses to determine if they are consistent with this constant Q. It can also be viewed as a means of estimating this Q from velocity data pairs. If the $1/Q$ terms on the right-hand side are dropped, as is suitable for Q much larger than 1, we arrive at the common operational definition of Q which can be used to solve directly for it, given c. Here c will be taken as a constant at 3.7 km/s, the speed of the main peak.

Estimates of Q have been found for all adjacent pairs of records along with the extreme pair. In each case the velocity spectra ratio has been corrected for instrument response [*Perret*, 1967] using the frequency domain response function of the sensors. These effects of these corrections on Q estimates are small. Figure 4 shows the series estimates of effective Q obtained using (1) with the Salmon velocity data records for the five adjacent pairs from the six ranges of 166, 225, 276, 318, 402, and 660 m. Figure 5 gives the overall Q estimate for the extreme pair at 166 and 660 m. The resulting effective Q values are remarkably similar, especially for the first, last, and extreme pairs. For each case, Q falls noticeably as the frequency approaches zero. Q generally passes through a value of 20 at about 100 Hz, passes through 10 at a few tens of hertz, and is generally 5 or less near the corner frequency of 6 Hz. The two record pairs involving the sensor at 276 m show a different behavior, especially at high frequencies. As shown in Appendix A, the reduced velocity potential for this record has significantly less high-frequency content than the other five. This record is not representative even though the time domain character appears typical.

There appears to be no significant difference between the initial and the final record pair estimate for Q, especially at frequencies near the corner. However, the results do consistently indicate a dependence on frequency. To determine better if a Q independent of both frequency and strain can be adequate, the initial pulse at 166 m has been propagated using *Kjartansson*'s [1979] model for $Q = 10$ with a compressional speed of 3.7 km/s. This value of Q, by design, then gives a reasonable fit to the changes in the peak pulse amplitude as illustrated in Figure 6. The scaled pulse shapes which result from this hypothesis are given in Figure 7. They can be compared directly with the scaled Salmon data in

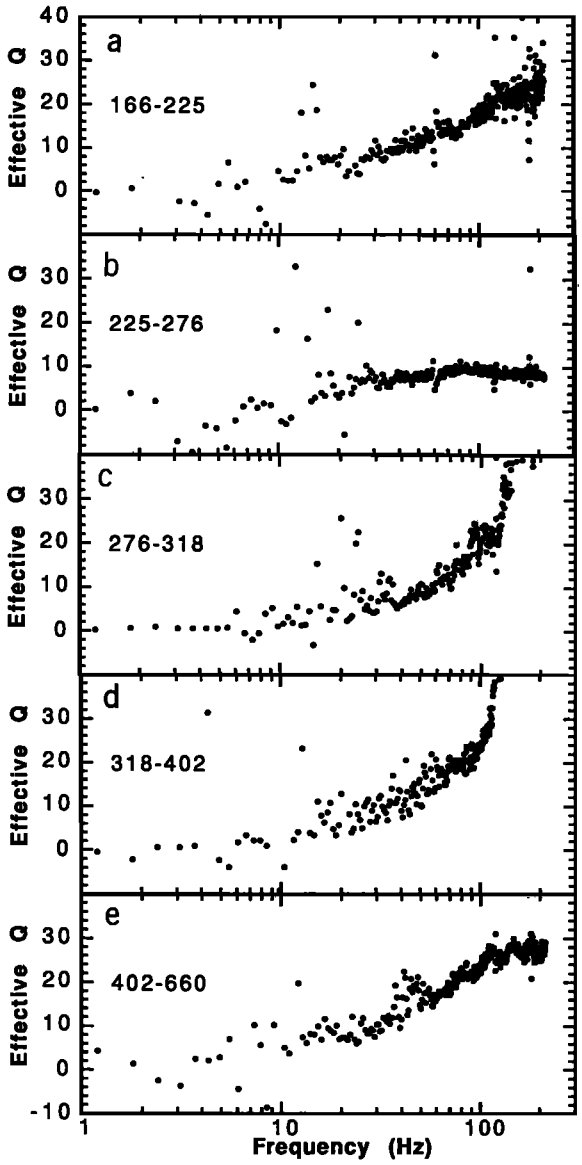

Fig. 4. Estimate of $Q(f)$ between ranges of (*a*) 166–225 m, (*b*) 225–276 m, (*c*) 276–318 m, (*d*) 318–402 m, and (*e*) 402–660 m.

Figure 3. The constant Q calculation gives pulses which become progressively broader and less peaked than the data. A constant Q is thus ruled out by the data.

Another hypothesis, which now seems more likely, is that a Q that is independent of strain level but that is a function of frequency can account for both amplitude and waveform

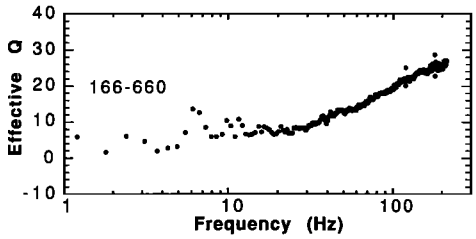

Fig. 5. Estimate of $Q(f)$ between the extreme record pair of 166 and 660 m.

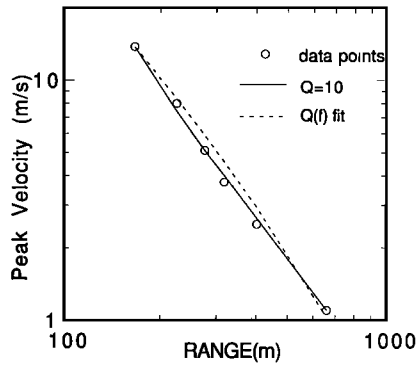

Fig. 6. Peak particle velocities for data, $Q = 10$, and frequency dependent Q.

variation. To test this possibility, the effective $Q(f)$ behavior for the pair of records at the extreme ranges shown in Figure 5 is replotted in Figure 8 as $1/Q$ versus frequency along with an approximate fit to the data using a convenient functional form which resembles the data (but which has no theoretical significance):

$$1/Q = 0.038[1 - \exp(-\alpha f)] + 0.20 \exp(-\alpha f) \quad (2)$$

Here $\alpha = 0.0266$ Hz^{-1} gives the best fit. This function is similar to that used by *Gupta and McLaughlin* [1989, Figure 8]. Figure 6 shows the peak amplitude variation while Figure 9 gives the scaled waveforms which result from using the 166-m Salmon pulse as a source and propagating with a frequency dependent Q and constant wave speed using (1) for Fourier synthesis. This gives a fair fit to peak amplitude decay, as seen in Figure 6. It provides a good fit to the peak width and sharpness. This indicates that if the data are produced by a linear Q, it must be frequency dependent. However, the precursor seen on each of the original data records is not adequately represented by this simple linear model.

The main purpose of using the Salmon data is to determine if they can rule out linear attenuation. Figures 4*a* and 4*e*, providing estimates of Q at the widest separation of ranges available, do not show manifest differences which would clearly demonstrate nonlinear behavior. However, there does appear to be a mild tendency for larger attenuation at smaller ranges, but given the scatter of the data, especially at low frequencies, it is difficult to measure. The data from adjacent sensor pairs are not adequate to define Q fully as a function of frequency at lower frequencies. However, it is possible to use (2) to define a candidate frequency dependence and then fit the data by finding a multiplicative factor to give a best fit. This has been done using the results of Figures 4*a* and 4*e*. If linear attenuation is operative, we expect all pairs to have the same Q, aside from experimental variation. The curves of $1/Q$ which result from this for the 166–225, 166–660, and 402–660 m intervals are shown in Figure 10. The decrease in $1/Q$ over the range interval covered is about 20% which can be compared with about 40% from the range$^{-1/2}$ falloff found by *Gupta and McLaughlin* [1989].

There are uncertainties in the $1/Q$ values found which must be considered. These are due to both absolute amplitudes and waveforms resulting from corrections needed for the original data. Mild fluctuations of corrected peak ampli-

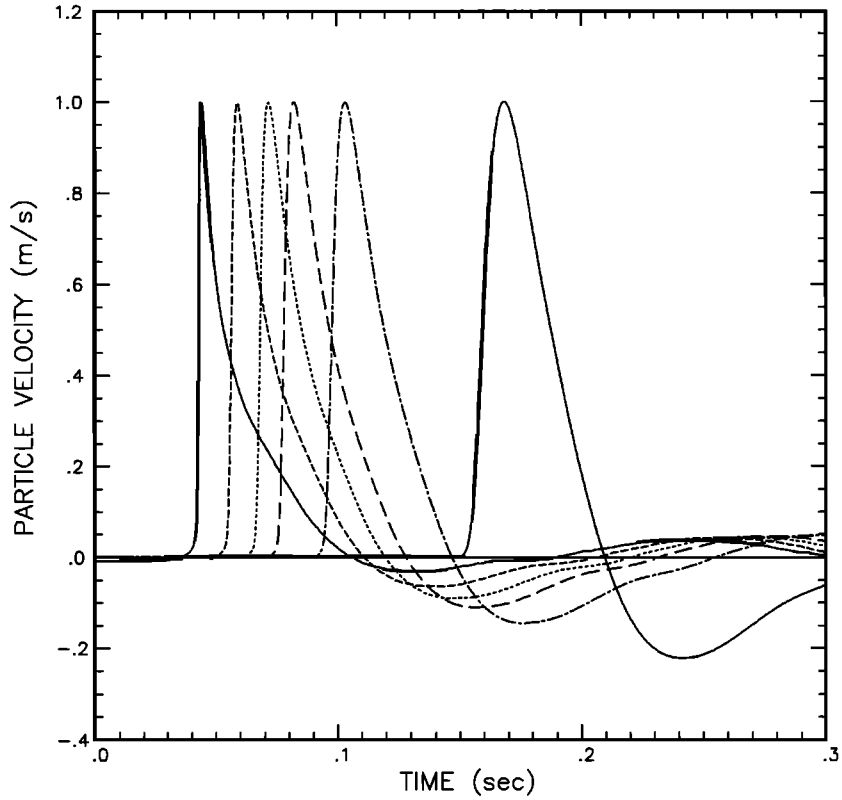

Fig. 7. Scaled pulse shapes for a frequency independent Q of 10.

tudes about a mean variation with range, which could result from inappropriate corrections or errant calibration of sensors, are evident in Figure 11. *Perret*'s [1967] and the uncorrected values are also shown. Even within the selected data set there are fluctuations of about 5%, and considering Perret's values and those not selected, as given in Appendix A, the uncertainty in the amplitudes is perhaps 5–10%. Figure 12 shows the range of variation of $1/Q$ estimates which will be produced given that one of the amplitudes used in the 166–660 sensor pair is changed uniformly by 5 and 10% as could result from an overall amplitude scaling of the record. The $1/Q$ estimates then appear quite stable against overall amplitude uncertainty at high frequencies but tend to become unstable below about 10 Hz. Uncertainties in the frequency domain reduced velocity potentials (RVPs) associated with correction of the corrupted data records, as discussed in Appendix A, have a character much like that seen for amplitude uncertainties. The high frequencies are only modestly affected while the frequencies below the corner are much more substantial. This difference in frequencies is reflected in Figure 8 where the Q estimates become spread out at low frequencies. Both waveform and overall amplitude uncertainties are significant around the dominant frequencies of the Salmon pulses. However, we note that the Q estimates taken from the corrected records consistently indicate a Q which decreases with decreasing frequency. The ability to fit all the observed waveform changes with a particular frequency dependent Q, as shown in Figure 8, indicates that this frequency dependence is a robust feature of the analysis. Furthermore, the amplitude of this Q, which is about 5, near the corner frequency must be approximately correct since the amplitude decay is largely determined by the attenuation around the dominant frequencies.

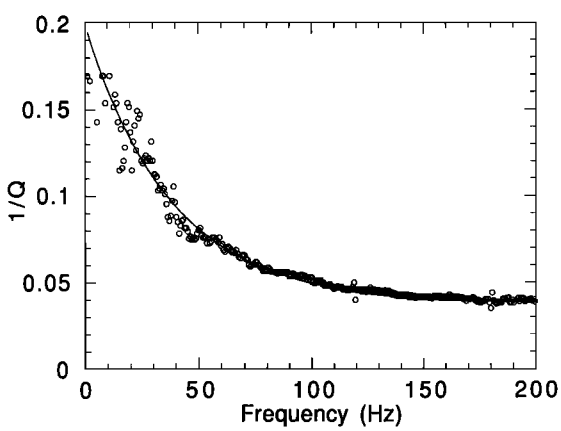

Fig. 8. Mean $1/Q$ between ranges from 166 to 660 m and a fit to the behavior.

Precursor Analysis

The technique which we have used is that of taking the observed Salmon initial velocity at small range (166 m) as a source and comparing the resulting pulses as they are propagated through material subject to candidate constitutive relations. The results are compared with observed signals at larger ranges. For any constitutive relation the effective Q associated with the attenuation may be determined, but it must be emphasized that nonlinear attenuation

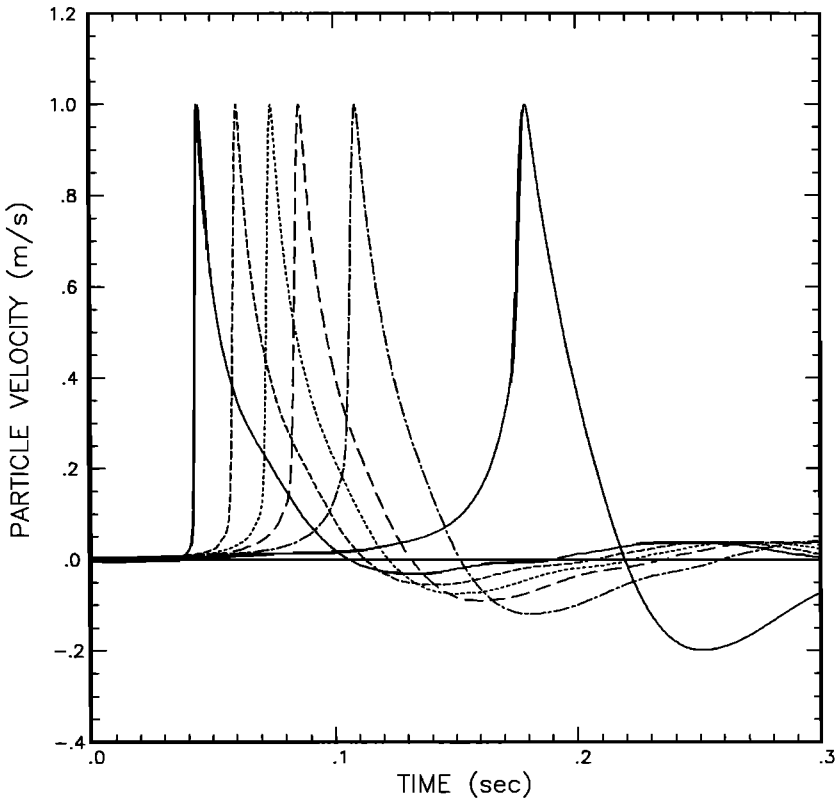

Fig. 9. Scaled pulse shapes for a specific frequency dependent $Q(f)$.

cannot be properly described by a Q function. The fundamental comparison of the data with calculations is not in terms of the Q but in terms of reproduction of waveform including both amplitude and shape.

As an equation of state hypothesis which can be consistent with the Salmon data, consider a medium for which the shear modulus permanently decreases (or at least does not recover until the pulse is past) upon having a critical strain threshold exceeded; the compressional modulus before and after exceeding the strain threshold reflects the compressional speeds at the beginning and peak of the Salmon pulses, respectively. This will be referred to as a shear failure model. Depending upon the relation between the compressional and the shear moduli, complete shear failure may occur, meaning that the elastic shear modulus μ goes to zero. For the example used in this discussion the compressional speed decreases to 80% of its original value. We have taken the Lamé constants λ and μ to have a ratio of 2. Thus a decrease of the compressional speed, $[(\lambda + 2\mu)/\rho]^{1/2}$, where ρ is the density, of 20% corresponds to reducing μ to about 38% of its elastic value when λ is held fixed. Note that the reduction of modulus at a fixed strain is consistent with scaling since the strain is a unitless quantity and there is no rate dependence. The scaling restriction does require that the relaxation time of the modulus change be short compared with any representative time scale of the data; we take the transition to be instantaneous. In order to determine the effect on the pulse propagation we use the observed Salmon velocity at 166 m as the source. These calculations were

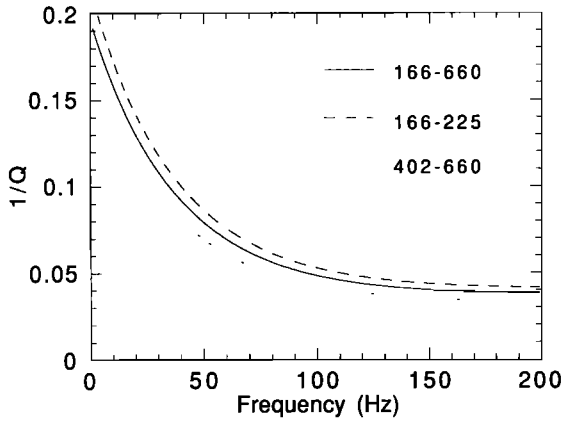

Fig. 10. Fits of $1/Q$ for 166–225, 166–660, and 402–660 m ranges.

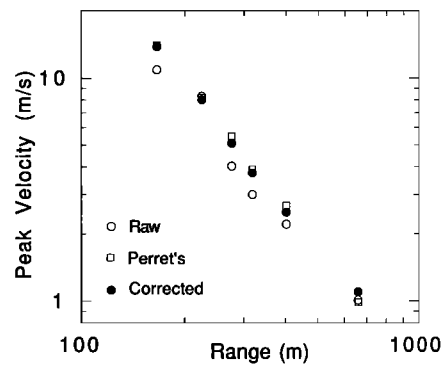

Fig. 11. Peak particle velocities for corrected data, for *Perret*'s [1967] analysis, and for no corrections.

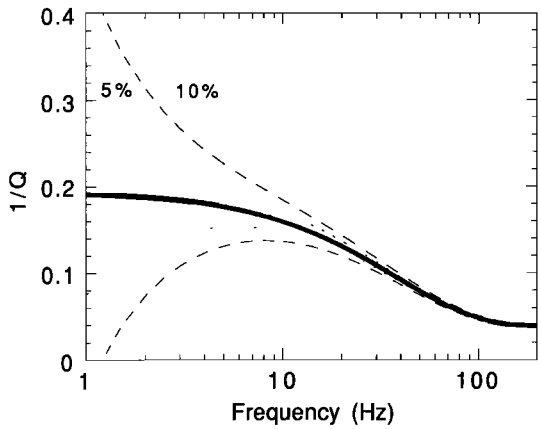

Fig. 12. Estimate variations of $1/Q$ for 5 and 10% velocity amplitude variation.

carried out using a standard finite difference method as illustrated by *Wilkins* [1964] with a uniform medium extending well past the most distant sensor location.

As an initial effort, the elastic threshold was taken at a compressional strain of 10^{-4}; the resulting pulse sequence at the ranges to observation stations for Salmon is as shown in Figure 13. Note that the character of the calculated precursor is much like that seen experimentally, in Figure 2, in that the leading feature is drawn out, the transition to the main pulse takes place at a constant amplitude, and the peak now moves at a significantly lower speed. Still the amplitude of the main peak does not decrease as quickly as the data indicate.

When the modulus decreases, the elastic energy in the pulse also decreases in a manner approximately proportional to the square of the compressional wave speed. Since the modulus reduction is permanent, this energy is lost to the pulse and goes into heating the medium. For the parameter used, over a full cycle for which most of the pulse exceeds the critical strain, approximately one third of the original elastic energy will be lost. This corresponds to an effective Q of about 13 for peak strains well in excess of 10^{-4} (for small strains less than this threshold, which occurs near 1000 m/kt$^{1/3}$, there will be no loss). This value of Q is far less than that expected for very small strain (*Gupta and McLaughlin* [1989] give $Q > 300$ for Sterling at strains of 10^{-5}), but it is more than the 5–10 seen for Salmon attenuation. The addition of a moderate level of linear attenuation consistent with that seen for small to moderate strains in other experiments will improve the agreement (for example, the New England Research (NER) [*Coyner*, 1987] data suggest $Q \approx 20$). More importantly, the use of a partial shear failure mechanism will automatically terminate once the pulse weakens so that the peak strain falls below the critical strain threshold value. This will produce a sharply changing effective Q in a manner suggested by the Cowboy data.

The attenuation from partial shear failure alone does not produce an amplitude for the pulse at 660 m which is as small as that seen experimentally. More attenuation can be added to attempt to match the data better by employing a linear Q of sufficient value. A method of inclusion of a linear absorp-

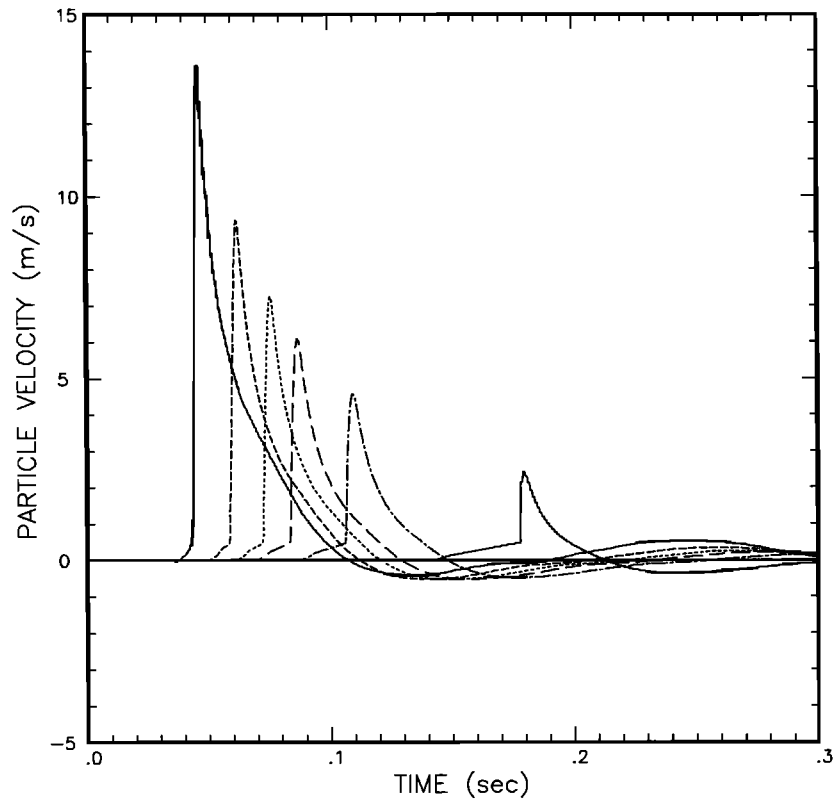

Fig. 13. Pulses at Salmon ranges for finite difference calculation of partial shear failure at compressional strain threshold of 10^{-4}.

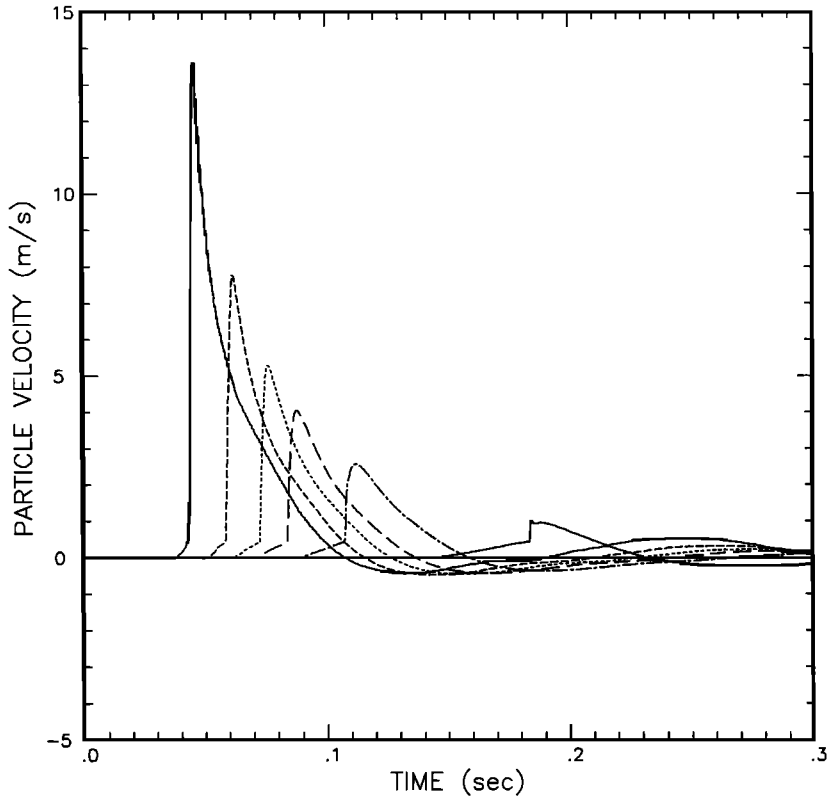

Fig. 14. Pulses at Salmon ranges for finite difference calculation of partial shear failure at compressional strain threshold of 10^{-4} and a linear Q of 10.

tion band Q in time-stepping finite difference methods has been demonstrated by *Day and Minster* [1984] through use of Padé approximants. Our application of this method is outlined in Appendix B. This formalism was employed using a target Q of 10 with a range of half-amplitude frequencies of 1–100 Hz (Q rises above 20 beyond these values). The sequence of pulses that results using both the partial shear failure and a linear Q of 10, starting with the Salmon pulse at 166 m, is shown in Figure 14. The amplitudes for the main peaks now are in substantial agreement with the data, and the length and amplitude of the precursor are also reproduced fairly well. There remains a very abrupt transition from precursor to main pulse which is clearly sharper than the experimental data. In order to avoid the abrupt transition between precursor and pulse a range of the threshold for the shear failure has been added to the model. This allows a variation of failure threshold values of compressional strain over a range of ±30% with a constant probability about the 10^{-4} value. Each cell in the finite difference calculation is given its own threshold which is randomly chosen on this basis. The set of pulses at the Salmon instrument ranges then calculated is given in Figure 15. The result is a smoother transition from precursor to main pulse in a manner which is quite similar to the actual Salmon data shown in Figure 2. While it is possible to achieve a detailed fit to the data using further such refinements, this is not a very meaningful thing to do since the mechanisms are not understood to the required level of detail. The important point is that it is possible to reproduce the data to a substantial degree using only a few physically based parameters to describe the thresholded partial shear failure. *Rimer and Cherry* [1982] have shown that it is possible to reproduce the Salmon data, including the precursor, using a shear strength limit which is variable. The yield strength is initially weak but then strengthens and weakens again through quadratic work hardening.

Discussion

A free-field ground motion data set, chosen for internal consistency from six stations from the Salmon nuclear explosion at ranges from 166 to 660 m, has been examined. This set has been used to determine if the associated attenuation of amplitude and distortion of pulse shape imply operative nonlinear effects in this moderate strain regime with strains of 10^{-3} to 10^{-4}. This is done by attempting to account for the data using a strictly linear description such that a failure would indicate the alternative, nonlinear behavior. It is found that within the limits of accuracy of the experimental data and by ignoring the elastic precursor, it is possible to account for these Salmon data, taken by themselves, using a strictly linear attenuation model with a frequency dependent Q which is of the order of ten for dominant frequencies. However, within the uncertainties there is a slight tendency for the attenuation to decrease with decreasing strain. There is about a 20% change in effective $1/Q$ over the range from midway between the extreme sensor pairs of 195–531 m. Furthermore, the experimental decay of peak velocity amplitudes is initially a bit faster than predicted with a frequency dependent Q model which again hints that there may be modest nonlinearities. However, because of the modest level of the change and the scatter of

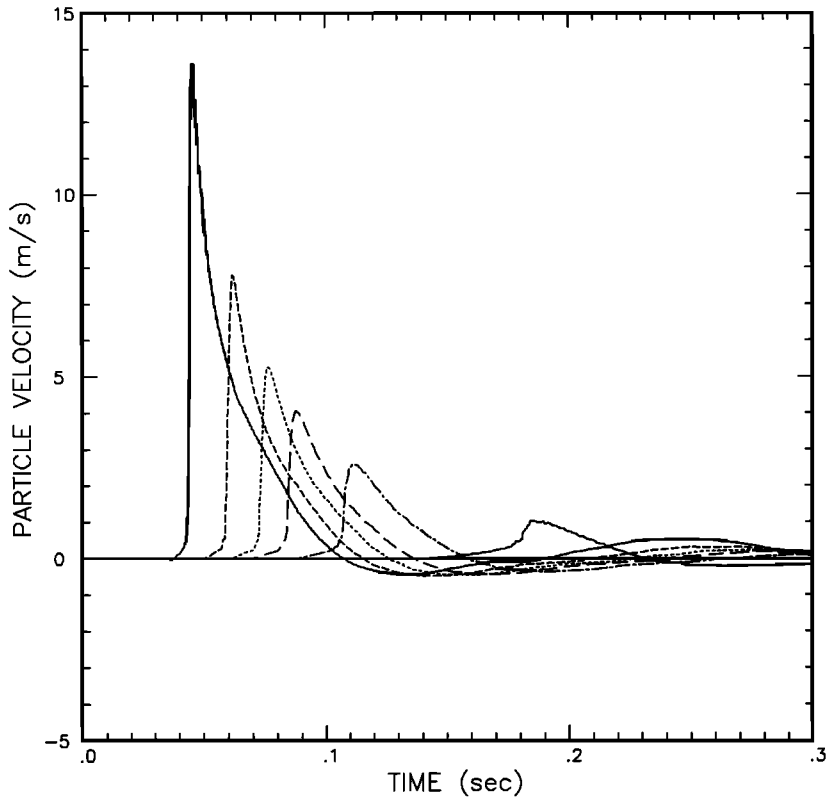

Fig. 15. Pulses at Salmon ranges for finite difference calculation of distributed partial shear failure and a linear Q of 10.

the data at dominant frequencies below 10 Hz, it is not possible to say firmly that these data illustrate nonlinear effects at the dominant frequencies of the Salmon waveform. Above about 25 Hz the data do indicate that the effective $1/Q$ decreases slowly with decreasing strain.

Gupta and McLaughlin [1989] used a larger but less selected Salmon data set based chiefly on velocity sensors and employed methods similar to those employed here. They indicate that the effective $1/Q$, averaged over the 1- to 25-Hz band, does decrease noticeably with decreasing strain, by about 40% over the range from midway between the extreme sensor pairs of 195–531 m. However, a Q independent of range is very nearly within their quoted limits of uncertainty. Other of *Gupta and McLaughlin*'s [1989, Table 2] results indicate that when different data sets from different sensors are used, the $1/Q$ estimates over 1–25 Hz, averaged over all ranges, vary from 0.09 to 0.21, which is an amount comparable with the 40%. Their 1- to 25-Hz $1/Q$ value quoted for use of all velocity and acceleration, records, both vertical and horizontal, averaged over all ranges is 0.16 ± 0.08. This again covers the extent of the calculated variation with range.

We believe that the Gupta and McLaughlin study and current studies provide essentially the same result. They indicate a probable modest decrease of attenuation over the range available from the Salmon data but with uncertainties which cannot rule out a strictly linear interpretation of the attenuation from this experiment alone. However, it seems clear that the attenuation at lower strains, or greater scaled ranges, must decrease significantly to meet the much larger Q indicated by results seen for Sterling, Cowboy, and other data [*Tittmann*, 1983] at strains approaching 10^{-6}. Still, the Salmon data, taken by themselves, do not show the precipitous decline in attenuation with decreasing stain which is expected to occur in approaching this small strain limit. However, note that a linear but frequency dependent Q, which is clearly required for Salmon, is in distinct contradiction to the observed yield$^{1/3}$ scaling of a range of explosive pulse propagation experiments. This is another reason for believing that the attenuation seen for Salmon is actually nonlinear.

The elastic precursor seen in Salmon near-field, moderate strain, velocity data is reproduced rather well with the hypothesis of partial shear failure which is activated for the duration of the pulse when the compressional strain exceeds 10^{-4}. This also gives an attenuation mechanism which accounts for much of the energy loss seen in the decay of pulses from Salmon with range. However, the overall attenuation produced is not quite adequate to account for that seen in the data. The addition of a broad linear absorption band attenuation, which is active over much of the significant frequency range appropriate to Salmon and which has a Q of 10, then provides a propagation model which nearly reproduces the signals at ranges beyond 166 m when the observed signal at this range is used as the source. Furthermore, this threshold mechanism provides a transition toward a more modest attenuation at small strains which is required to be consistent with Cowboy data; when applied to different yield events in salt, it will produce simple scaling as observed over a wide range of explosive events. While there is no assurance that this mechanism applies in other than the salt medium, *Perret* [1967, pp. 89–91] points out that elastic precursors of a similar character have been seen in underground test pulses in both alluvium and dolomite. The fact

that the reduction in compressional wave speed is attributed to shear failure, rather than to the alteration of some other material property, is largely a matter of consistency with past thinking on modes of material behavior; there is no direct experimental link to shear properties. The general agreement with data which results could just as well have been produced by any method which reduces the compressional modulus in the required amount.

To summarize the results, it appears that the details of the Salmon waveform shape and amplitude data can be accounted for by a linear Q of approximately 10 in conjunction with a nonlinear partial shear failure mechanism which will cease to be operative at strains less than 10^{-4}. However, this model is not complete in that it does not give a full transition to the much smaller attenuation expected as the strains approach the linear limit of perhaps 10^{-5} to 10^{-6}; the Salmon data do not provide information on this transition. Even though these data cannot rule out a linear behavior for the nonprecursor aspects of the propagation, we suspect that the attenuation is actually dominated by nonlinear effects which happen to be able to be represented by an effective Q function over this limited strain range. A single experimental data set which clearly demonstrates the transition to linear behavior for explosively generated pulse remains to be generated.

Appendix A: Salmon Data Correction and Selection

Data records for Salmon were taken by both velocity and acceleration gages, oriented either horizontally or vertically [*Perret*, 1967]. A sketch of the layout of gages has been reproduced by *Gupta and McLaughlin* [1989] and *Rogers* [1966]. The horizontal gages were aligned either radially from the source or transverse to this direction. The raw acceleration data allow determination of velocity by integration. Problems arise as illustrated by the example in Figure A1. The raw velocity generally not only does not go to zero but also increases at a constant rate; the perpetual increase is due to a postshot nonzero baseline for the acceleration instruments produced by alteration of calibration. (Velocity sensors also show postshot baseline shifts.) This must be corrected by altering the acceleration baseline at late times to a nonzero constant and then subtracting a linear velocity trend shown by the dashed curve. This baseline correction is not appropriate before the pulse arrives, so it must begin during the pulse. The corrected velocity baseline must go to zero at early times, but it is impossible to do this uniquely. As indicated in the figure, we take the baseline shift to begin at the pulse peak. The difference between the corrected baseline and the raw record gives a corrected velocity which goes to zero at late times. There is a problem beyond this because even when the late-time acceleration is forced to zero, the late-time velocity, while now constant, is generally not zero. This may be a result of clipping [*Perret*, 1967, p. 39] of the acceleration peak due to inadequate instrument response or to inadequate bandwidth in recording.

It is impossible to correct the clipping difficulty in a unique manner; the only requirement is that the velocity return to zero at late time. It appears to be possible to make corrections in a consistent manner, which leads to results quite close to those given by Perret. While Perret does not discuss the details of his corrections, he had access to complete

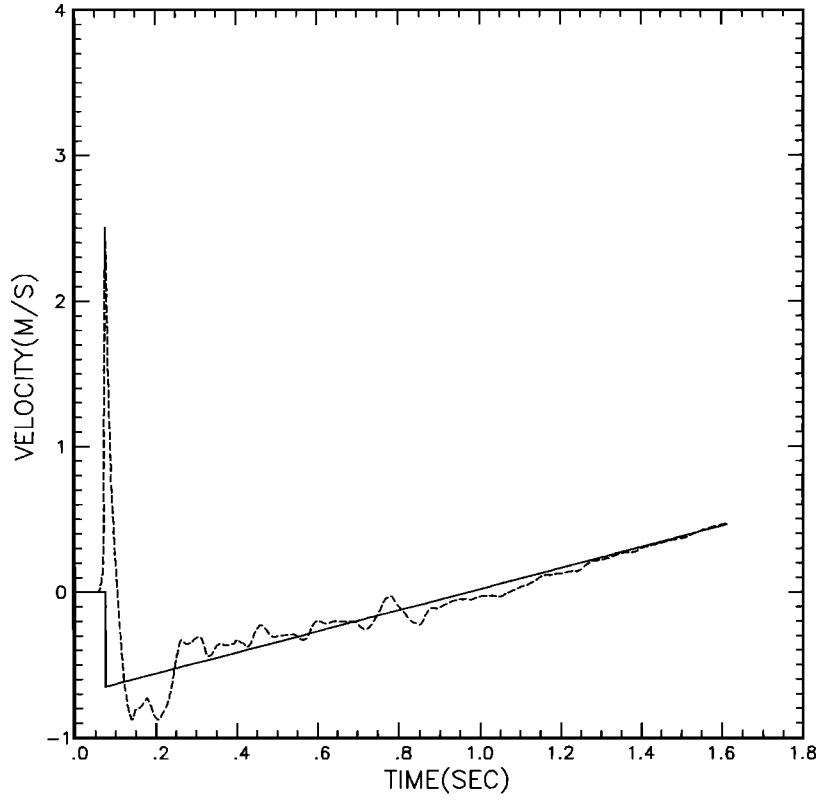

Fig. A1. Uncorrected E14-20AR record with proposed baseline.

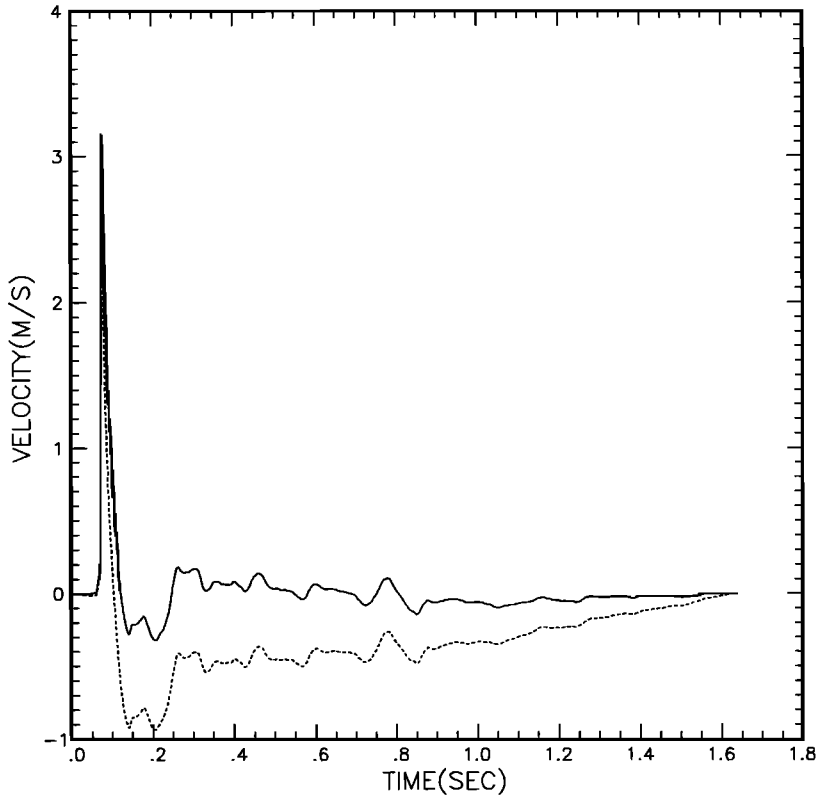

Fig. A2. Corrected E14-20AR record using a clipping correction (solid curve) and a simple baseline correction (dotted curve).

instrument performance data as well as substantial insight into experimental details. He took advantage of those stations which had both acceleration and velocity instruments to define corrections which made the two results quite similar. In the absence of further information we have chosen to correct the data as follows. As discussed in the paragraph above, a postpeak velocity baseline was defined after the once-integrated raw acceleration records are fit at late time with a straight line from the last data point used (at 1.6384 s) back to the time of the initial positive peak with a slope chosen to give a behavior at times later than the peak consistent with that shown by Perret. For points later than the peak the difference between the baseline and the raw data provides corrected values. The velocity points before the peak were then altered by scaling all the prepeak data by a constant factor, ranging from 0.96 to 1.27 over the six records used, chosen to make the corrected velocity peak continuous. This amounts to uniformly scaling the entire initial acceleration positive phase pulse to compensate for clipping. It assures that the velocity is continuous and that the leading edge retains its original steep character. The mild discontinuity in the first derivative exactly at the velocity peak cannot be seen by merely looking at the resulting plotted velocities because of its modest extent and the noise on the velocity signal. The result of all this is an effective change in the raw acceleration records which compensates for both the baseline shift and the peak clipping. The resulting peak amplitudes are given in Figure 6 in the main text. This production of corrected records is obviously both subjective and ad hoc. The justification is that the resulting records are very much like those given by the best estimates of the original experimenter, Perret. Also, since we are primarily interested in comparing records at a sequence of stations, the use of this uniform procedure will change the records in a consistent manner so that the spectral pairs will change in comparable ways and the ratios may be relatively stable. However, this is conjectural, and the real test is in the consistency of results.

A measure of the data record correction effect on conclusions for attenuation can be found by comparing the variation in reduced velocity potential resulting from different approaches to handling the data. Figure A1 shows the raw data for an example which was selected for use in this analysis. This once-integrated radial acceleration was corrected in the manner described above to yield a record with the obvious effects of baseline shift and clipping removed, giving the result in Figure A2. In this same figure the results of the less complex but clearly imperfect correction procedure are also given. This alternate method, which we call a simple baseline adjustment, consists of subtracting a single baseline formed by simply joining the first and last points with a straight line. This guarantees that the initial and final velocities will be zero, but it will obviously leave residual effects of both clipping and baseline shifts. Figure A3 shows the RVPs which result from the use of our correction, from the simple baseline adjustment, and for no correction at all. At frequencies above about 6 Hz, which happens to be the corner frequency, the methods yield very similar results. The variation among the methods is only about 25% in spite of the rather extreme nature of the alternate techniques. This variation is comparable with the fluctuation in the individual RVPs as a function of frequency. In view of the obvious

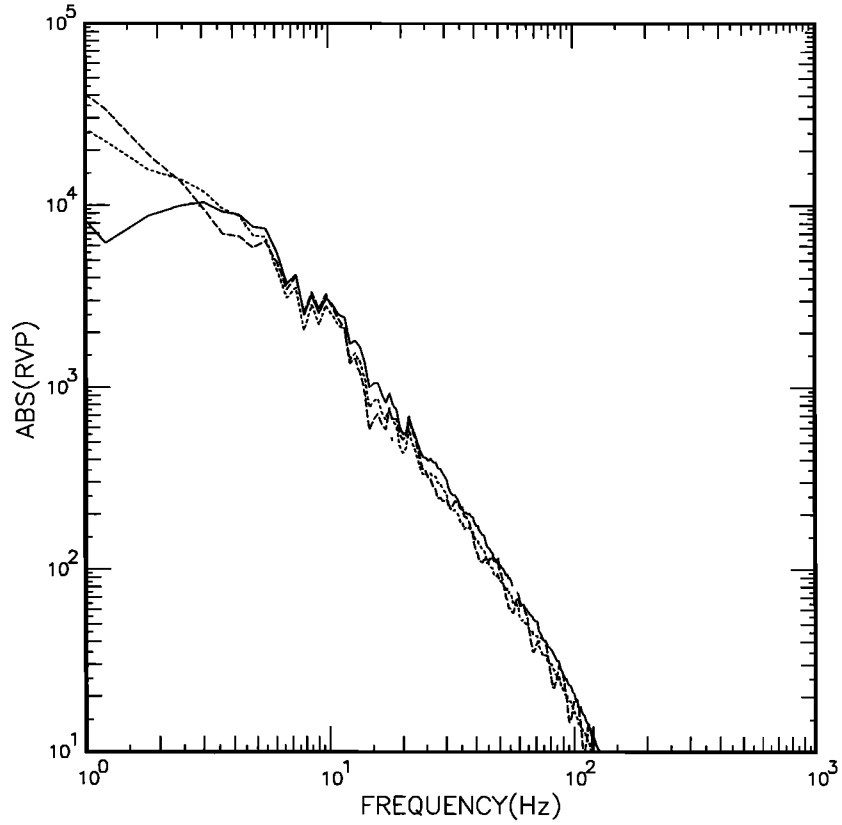

Fig. A3. RVPs for E14-20AR record, corrected for clipping (solid curve), corrected with simple baseline (dotted curve), and uncorrected (dashed curve).

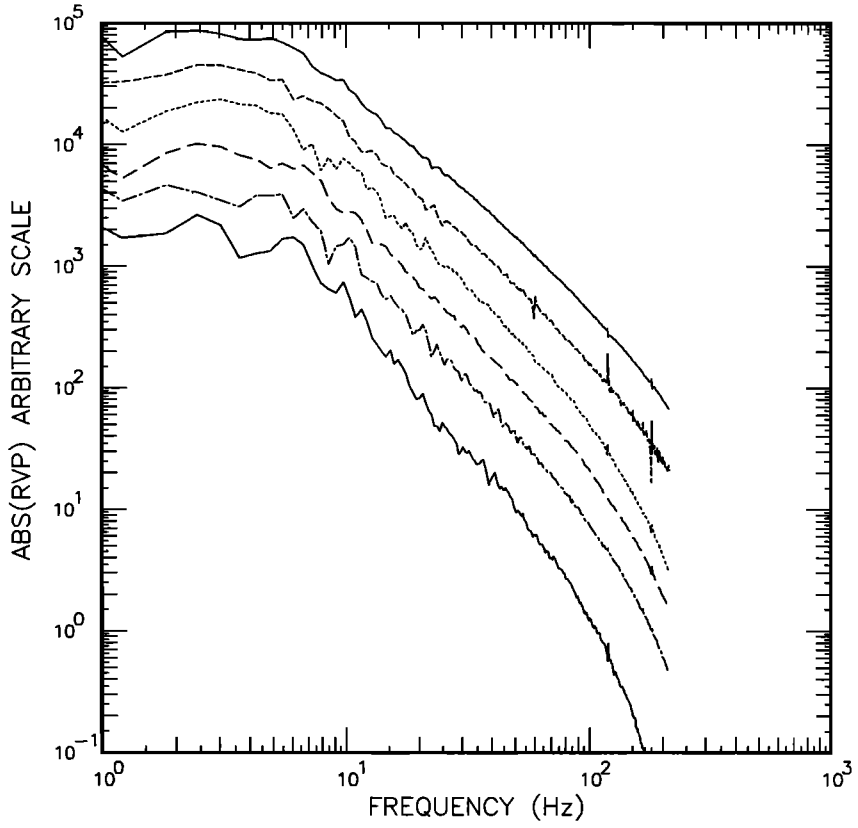

Fig. A4. RVPs for six corrected records stacked with a constant offset of a factor 2.

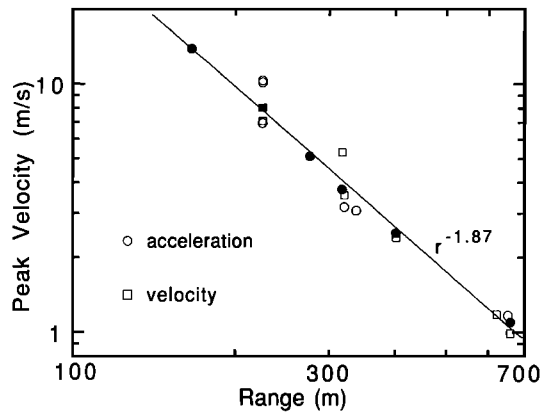

Fig. A5. Corrected peak velocities for available acceleration and velocity records. Solid symbols indicate those selected.

problems with either no correction or a simple baseline adjustment, this variation level probably should be regarded as an upper bound on the uncertainties associated with correction methods. At frequencies below about 3 Hz there is significant divergence among the methods. However, our corrected RVP shows evidence of turning over near the corner frequency which is consistent with the behavior seen for all records shown in Figure A4. It is to be expected that some methods of correcting the records will lead to substantial variation on approaching the low-frequency behavior. At a fixed range the low-frequency limit of the RVP is proportional to the final particle displacement which is small compared to the maximum displacement. Failure to correct a peak properly will have a large effect on the net displacement. The impact of these correction uncertainties on the conclusions of this paper is given in the main text. The RVP found for this particular record is representative of those for the other selected records.

We have attempted to select a compatible set of records which satisfy, as well as possible, criteria making them suitable for comparison by spectral ratio. These are that they (1) come from only a single type of instrument (acceleration or velocity, radial or vertical), (2) be from stations which are fairly uniformly and widely spaced, (3) be correctable in a consistent way to reproduce *Perret*'s [1967] results, and (4) be as internally consistent as possible in amplitude and waveform.

On the basis of these criteria a set of six records were selected for study that included those at ranges from 166 to 660 m. First, vertical motion was not used since the radial component was generally much the larger of the two. Of the 20 radial acceleration and velocity records available to us, two were known to be incorrectly oriented and so were rejected. Corrected peak velocities, trigonometrically adjusted to give the spherical radial velocity, for the remaining 18 are plotted on Figure A5. The acceleration and velocity records are distinguished, and those selected are indicated by solid symbols. First, note that the stations at 166 and 276 m have only acceleration records available (E14-27AR and E14-20AR, respectively). We thus have chosen to use acceleration records where possible. The acceleration stations at 225 m show peaks which are rather far from the general trend. The closest candidate (E14-32AR) has a corrected peak at 7.0 m/s and has unusually large oscillations in its postpeak waveform. Perret gives a significantly different peak of 7.7 m/s. Consequently, we have not used this record but have taken a velocity record (E14-20UR) at this range instead. Only a single acceleration record at 402 m is available, and its amplitude is nearly in line with those chosen already. Near 318 m there are three acceleration stations available. The one which most closely falls along those chosen in E6-27AR which is at the same depth as the shot. Finally, at 660 m there are two acceleration stations which show quite similar results. The E11-34AR result is slightly closer to following the power law falloff found for the data as a whole which is given by Perret as $r^{-1.87}$ and shown in Figure A5.

The available full data records extend out to about 5 s past the explosion and consist of values every 0.2 ms. It was found that after about 1.5 s the records showed no further significant contribution, so the data were truncated at 1.6384, conveniently giving 8192 data points for each reduced record.

Appendix B

Day and Minster [1984] have shown how to include an arbitrary linear Q function in time-stepping calculations. For an absorption band an analytic solution is available. An outline of their methods, as generalized to the spherical case, is given here.

For a single normalized relaxation function $m(t)$ the stresses and strains are related by

$$\sigma_r = (\lambda+2\mu)\int \dot{m}(t-\tau)\varepsilon_1(\tau)\,d\tau + 2\lambda\int \dot{m}(t-\tau)\varepsilon_2(\tau)\,d\tau \tag{B1}$$

$$\sigma_\theta = (2\lambda+2\mu)\int \dot{m}(t-\tau)\varepsilon_2(\tau)\,d\tau + \lambda\int \dot{m}(t-\tau)\varepsilon_1(\tau)\,d\tau \tag{B2}$$

Here $\dot{m}$ is the time derivative of m and the strains are

$$\varepsilon_1 = \partial u/\partial r \tag{B3}$$

$$\varepsilon_2 = u/r \tag{B4}$$

where u is displacement. Generally, one could have two different relaxation functions (e.g., bulk and shear), but we shall not consider this possibility. The λ and μ are the usual Lamé constants which are now the unrelaxed or high-frequency moduli of the medium. The stresses can be written in terms of Q-corrected strains, e, as

$$\sigma_r = (\lambda + 2\mu)e_1 + 2\lambda e_2 \tag{B5}$$

$$\sigma_\theta = (2\lambda + 2\mu)e_2 + \lambda e_1 \tag{B6}$$

Day and Minster have shown how to express the e_i in terms of the ε_i:

$$e_i = \int \dot{m}(t-\tau)\varepsilon_i\,d\tau \tag{B7}$$

using a sequence of Padé approximants to write the integral equation as a differential relation. For an absorption band attenuation with relaxation times between τ_1 and τ_2 and with

a flat spectrum, they show that the integral relation can be replaced by

$$e_i(t) = \varepsilon_i(t) - \sum_{k=1}^{M} \zeta_i^k(t) \tag{B8}$$

where

$$\frac{d}{dt}\zeta_i^k + \nu_k \zeta_i^k = \left(\frac{\tau_i^{-1} - \tau_2^{-1}}{\pi} W_k Q_0^{-1}\right)\varepsilon_i(t) \qquad k = 1, \cdots, M \tag{B9}$$

Here Q_0 is the target Q in the absorption band,

$$\nu_k = \frac{1}{2}[l_k(\tau_1^{-1} - \tau_2^{-1}) + (\tau_1^{-1} + \tau_2^{-1})] \tag{B10}$$

where the l_k are the abscissas and W_k are the weights for M-point Gauss-Legendre quadrature. The index M is that of the Padé approximant. As M increases, the solution converges to the analytic result, which in the frequency domain is

$$-i\omega\tilde{m}(\omega) = 1 - \frac{2}{\pi Q_0}\ln\left[\frac{\tau_2}{\tau_1}\left(\frac{1+\omega^2\tau_1^2}{1+\omega^2\tau_2^2}\right)^{1/2}\right] - \frac{2i}{\pi Q_0}\tan^{-1}\left[\frac{\omega(\tau_2 - \tau_1)}{1+\omega^2\tau_1\tau_2}\right] \tag{B11}$$

This analytic form allows the propagation of any pulse. By defining a reduced displacement potential (RDP) ϕ by

$$u(r, t) = \frac{\partial}{\partial r}[\phi(r, t)/r] \tag{B12}$$

and by applying the equation of motion for spherical symmetry

$$\rho\frac{\partial^2 u}{\partial t^2} = \frac{1}{r^2}\left[\frac{\partial}{\partial r}(r^2\sigma_r)\right] - \frac{2}{r}\sigma_\theta \tag{B13}$$

in the presence of the relaxation function, (B1) and (B2) lead to this expression for advancement of the RDP from "a" to "r":

$$\phi(r, t) = \frac{1}{2\pi}\int d\omega\ \tilde{\phi}(a, \omega)\exp\left[-i\omega t + i\frac{\omega(r-a)}{\alpha(-i\omega\tilde{m})^{1/2}}\right] \tag{B14}$$

where $\alpha = [(\lambda + 2\mu)/\rho]^{1/2}$ is the unrelaxed compressional phase speed and the tilde indicates the Fourier transform. Using (B12) then gives a means of propagating a displacement or velocity pulse given a $\tilde{m}$ such as from (B11).

Kjartansson [1979] gives this relaxation function which provides constant Q:

$$-i\omega\tilde{m} = (\omega/\omega_0)^{2\gamma}\exp[-i\pi\gamma\ \mathrm{sgn}\ (\omega)] \tag{B15}$$

where the arbitrary constants are a reference frequency ω_0 and

$$\gamma = (1/\pi)\tan^{-1}(1/Q) \tag{B16}$$

The propagation of the RDP is given by

$$\phi(r, t) = \frac{1}{2\pi}\int \tilde{\phi}(a, \omega)\exp\left[-i\omega\left(t - \frac{r-a}{c}\right) - \frac{\omega(r-a)\ \mathrm{sgn}\ (\omega)}{2cQ}\right] d\omega \tag{B17}$$

where the phase speed c is a function of frequency:

$$c = c_0|\omega/\omega_0|^\gamma/\cos\ (\pi\gamma/2) \tag{B18}$$

Here c_0/ω_0^γ is an arbitrary constant which fixes the phase speed at an arbitrary reference frequency.

When the RDP is related to the velocity by (B12), the velocity pulse will propagate according to (1) in the main text.

Acknowledgments. This research has been sponsored by the Defense Advanced Research Projects Agency and monitored by the Geophysics Laboratory under contract F19628-87-C-0240. Helpful discussions with S. Day of San Diego State University, J. Murphy of S-Cubed, J. Trulio and N. Perl of Applied Theory, B. Tittmann and J. Bulau of Rockwell International, and R. Blandford of DARPA are acknowledged. We also wish to thank the reviewers for very helpful comments.

References

Ahrens, T. J., and G. E. Duvall, Stress relaxation behind elastic shock waves in rocks, *J. Geophys. Res.*, *71*, 4349, 1966.

Aki, K., and P. G. Richards, *Quantitative Seismology Theory and Methods*, pp. 170–182, W. H. Freeman, New York, 1980.

Coyner, K. B., Attenuation measurements on dry Sierra white granite, dome salt and Berea sandstone, *Rep. NER Contract 9092405*, New Engl. Res., Inc., Norwich, Vt., 1987.

Day, S. M., and J. B. Minster, Numerical simulation of attenuated wavefields using a Padé approximate method, *Geophys. J. R. Astron. Soc.*, *78*, 105, 1984.

Denny, M. D., A case study of the seismic source function: Salmon and Sterling reevaluated, *J. Geophys. Res.*, *95*, 19,705, 1990.

Gupta, I. N., and K. L. McLaughlin, Strain and frequency dependent attenuation estimates in salt from Salmon and Sterling near-field recordings, *Bull. Seismol. Soc. Am.*, *79*, 1111, 1989.

Kjartansson, E., Constant Q wave propagation and attenuation, *J. Geophys. Res.*, *84*, 4737, 1979.

Langston, C. A., Kinematics analysis of strong motion P and SV waves from the Sterling event, *J. Geophys. Res.*, *88*, 3486, 1983.

Larson, D. B., Inelastic wave propagation in sodium chloride, *Bull. Seismol. Soc. Am.*, *72*, 2107, 1982.

Masse, R. P., Review of seismic source models for underground nuclear explosions, *Bull. Seismol. Soc. Am.*, *71*, 1249, 1981.

McCartor, G. D., and W. R. Wortman, Experimental and analytic characterization of nonlinear seismic attenuation, *Rep. MRC-R-900*, Mission Research Corp., Santa Barbara, Calif., 1985.

McCartor, G. D., and W. R. Wortman, Nonlinear attenuation mechanisms in salt at moderate strain based on Salmon data, *Rep. AFGL-TR-89-0013*, Mission Res. Corp., Santa Barbara, Calif., 1988.

Minster, J. B., and S. M. Day, Decay of wave fields near an explosive source due to high-strain nonlinear attenuation, *J. Geophys. Res.*, *91*, 2113, 1986.

Mueller, R. A., and J. R. Murphy, Seismic characteristics of underground nuclear detonations, *Bull. Seismol. Soc. Am.*, *61*, 1975, 1971.

Murphey, B. F., Particle motions near explosions in halite, *J. Geophys. Res.*, *66*, 947, 1961.

Perret, W. R., Free-field particle motion from a nuclear explosion in salt, I, Project Dribble, Salmon Event, *Rep. VUF-3012*, Sandia Lab., Albuquerque, N. M., 1967.

Rimer, N., and J. T. Cherry, Ground motion predictions for the Grand Saline Experiment, *Rep. USC-TR-82-25*, S-Cubed Corp., La Jolla, Calif., 1982.

Rogers, L. A., Free-field motion near a nuclear explosion in salt: Project Salmon, *J. Geophys. Res.*, *71*, 3415, 1966.

Taylor, J. W., and M. H. Rice, Elastic-plastic properties of iron, *J. Appl. Phys.*, *34*, 364, 1963.

Tittmann, B. R., Studies of absorption in salt, *Rep. SC5320SRF*, Rockwell Int. Sci. Cent., Thousand Oaks, Calif., 1983.

Trulio, J., Simple scaling and nuclear monitoring, *Rep. ATR-78-45-1*, Appl. Theory, Inc., Los Angeles, Calif., 1978.

Von Seggern, D., and R. Blandford, Source time functions and spectra for underground nuclear explosions, *J. R. Astron. Soc.*, *31*, 83, 1972.

Wilkins, M. L., Calculation of elastic-plastic flow, *Methods Comput. Phys.*, *3*, 211, 1964.

Wortman, W. R., and G. D. McCartor, Nonlinear seismic attenuation from Cowboy and other explosive sources, in *Seismic Coupling of Nuclear Explosions*, vol. 2, edited by D. B. Larson, *Rep. UCRL-21086*, Def. Adv. Res. Proj. Agency, Arlington, Va., 1989.

G. D. McCartor, Department of Physics, Southern Methodist University, Dallas, TX 75275.

W. R. Wortman, Mission Research Corporation, P.O. Drawer 719, Santa Barbara, CA 93102.

(Received January 22, 1990;
revised June 25, 1990;
accepted August 6, 1990.)